



저작자표시-비영리-변경금지 2.0 대한민국

이용자는 아래의 조건을 따르는 경우에 한하여 자유롭게

- 이 저작물을 복제, 배포, 전송, 전시, 공연 및 방송할 수 있습니다.

다음과 같은 조건을 따라야 합니다:



저작자표시. 귀하는 원저작자를 표시하여야 합니다.



비영리. 귀하는 이 저작물을 영리 목적으로 이용할 수 없습니다.



변경금지. 귀하는 이 저작물을 개작, 변형 또는 가공할 수 없습니다.

- 귀하는, 이 저작물의 재이용이나 배포의 경우, 이 저작물에 적용된 이용허락조건을 명확하게 나타내어야 합니다.
- 저작권자로부터 별도의 허가를 받으면 이러한 조건들은 적용되지 않습니다.

저작권법에 따른 이용자의 권리는 위의 내용에 의하여 영향을 받지 않습니다.

이것은 [이용허락규약\(Legal Code\)](#)을 이해하기 쉽게 요약한 것입니다.

[Disclaimer](#)

의학박사 학위논문

Development of  
a neuro-angiography vascular phantom model

디지털 감산 뇌혈관조영술 팬텀 모델의 개발

울 산 대 학 교 대 학 원

의 학 과

신 재 전

Development of  
a neuro-angiography vascular phantom model

지도교수 이 덕 희

이 논문을 의학박사 학위 논문으로 제출함

2019 년 08 월

울 산 대 학 교 대 학 원

의 학 과

신 재 전

신재전의 의학박사학위 논문을 인준함

심사위원	최 충 곤	(인)
심사위원	김 진 형	(인)
심사위원	안 재 성	(인)
심사위원	김 범 수	(인)
심사위원	이 덕 희	(인)

울 산 대 학 교 대 학 원

2019 년 08 월

## 감사의 글

먼저 연구 수행 중 고비를 만날 때마다 멘토 역할을 해주시고 연구가 진전될 수 있게 도와주신 지도 교수님 이덕희 교수님께 감사드립니다. 유체실험을 수행할 때 도움을 주신 NIDD 실험실의 맹준영 선생님, 황선문 선생님, 최준호 선생님께 감사드립니다. 아울러 팬텀모형 제작에 도움을 주신 울산대학교 융합의학과 권재영 연구원님과 주식회사 시니의 이병준 대표님, 통계 처리를 도와주신 서울아산병원 임상의학 연구소 이지성 교수님, iFlow 프로그램 해석 및 특성에 대해 알려주신 Ziemens applicator 최영락 과장님께도 감사의 말씀을 드리고 싶습니다.

바쁘신 중에도 학위 논문 심사 과정에서 좀 더 완성도 있는 연구가 되도록 많은 조언을 해 주신 심사위원 교수님들께 감사드립니다. 더불어 학위논문 작성 과정 동안 저에게 관심과 도움을 주신 가톨릭대학교 의정부 성모병원의 교수님들께도 감사드립니다.

무엇보다 가족의 도움이 없었다면 이 연구는 진행되지 못하였을 것입니다. 항상 묵묵히 응원을 해 주었던 아내 윤희, 아버지, 어머니, 장인어른, 장모님, 그리고 지형, 하나, 예준에게 감사드립니다.

## ABSTRACT

**Background and Purpose:** For optimally performing cerebral digital subtraction angiography, it is important to know how the concentration of contrast agent changes with various contrast injection protocols. The purpose of this study was to design an *in vitro* intracranial arterial phantom flow system with a mimicking capillary system for studying changes in contrast medium concentration.

**Materials and Methods:** We obtained patient's 3D cerebrovascular anatomy data and created a cerebrovascular phantom model that was hollowed out in the shape of a patient's cerebral artery. Our phantom flow system comprised a cerebrovascular phantom model, an acrylic hollow cistern filled with sponge, a pump, an injection system, a pressure-monitoring system, a constant temperature bath, and a venous drainage container. A plastic cistern filled with sponge was used to mimic the cerebral capillary system. We defined the following groups: Type A, the mimicking capillary system was not incorporated into the phantom flow system; Type B, only plastic cistern was employed without filling with sponge; and Type C, plastic cistern filled with sponge was employed. To validate these phantom model groups, we compared iFlow contrast concentration–time curve pattern of a real patient with that of the phantom flow system. The following four parameters were adopted to analyze iFlow images: 1) maximum contrast concentration, 2) time to peak, 3) full width at half maximum, and 4) area under the curve (AUC).

**Results:** All four parameters considered for analyzing changes in contrast concentration for A, B, and C groups showed a serial increase in values. The maximum contrast concentration in Type A did not differ significantly from that in real patient (*p-value* = 0.168 in comparison with patient values). Among the four parameters, full width at half maximum and AUC in Type C showed maximum similarity with values obtained from the patient's contrast concentration–

time curve ( $p$ -value < 0.001 in comparison with patient values).

**Conclusion:** We demonstrated that the contrast concentration–time curve of a real patient could be simulated with the cerebrovascular phantom flow system by adjusting resistance of the phantom flow model through an acrylic hollow cistern filled with sponge. Our study on cerebrovascular phantom flow system also provided a methodological foundation for contrast study in catheter-induced cerebral arteriogram.

**Keywords:** capillary system, cerebral digital subtraction angiography, contrast, phantom

# CONTENTS

<b>ABSTRACT</b> .....	i
<b>CONTENTS</b> .....	iii
<b>LIST OF FIGURES</b> .....	iv
<b>LIST OF TABLES</b> .....	v
<b>LIST OF ABBREVIATIONS</b> .....	vi
<b>INTRODUCTION</b> .....	1
<b>MATERIALS AND METHODS</b> .....	3
Selection of a patient model .....	3
Image processing with iFlow .....	3
Construction of the cerebrovascular phantom model .....	4
Configuration of the cerebrovascular phantom flow system .....	9
Validation of cerebrovascular phantom flow system .....	11
Statistical analysis .....	13
<b>RESULTS</b> .....	14
<b>DISCUSSION</b> .....	18
Limitation .....	20
<b>CONCLUSION</b> .....	22
<b>REFERENCE</b> .....	23
<b>국문요약</b> .....	25



## LIST OF FIGURES

Figure 1. Region of interest at color coded digital subtraction angiography. ....	6
Figure 2. Construction of a cerebrovascular phantom. ....	7
Figure 3. A cerebrovascular phantom model with an artificial brain capillary system. ....	8
Figure 4. The entire cerebrovascular phantom flow system. ....	10
Figure 5. The four parameters which were adopted for analyzing iFlow images. ....	12
Figure 6. Comparisons among the four parameters for Types A, B, and C. ....	16
Figure 7. Comparisons between the iFlow contrast concentration–time curves of the original person and cerebrovascular phantoms. ....	17

## **LIST OF TABLES**

Table 1. The four parameters for contrast opacity temporal change in the types. ....	15
--	----

## **LIST OF ABBREVIATIONS**

**DSA** Digital Subtraction Angiography

**MCA** Middle Cerebral Artery

**ICA** Internal Carotid Artery

**ROI** region of interest

**TTP** time to peak

**AUC** area under curve

**CFD** computational fluid dynamics

## INTRODUCTION

To optimally perform cerebral digital subtraction angiography (DSA), it is important to understand the effect of various contrast injection protocols on the concentration of contrast agent. However, it is ethically inappropriate to inject contrast agents in a human body or repeatedly expose it to radiation. Ahmed et al.<sup>1)</sup> have performed some experiments to study the bolus geometry of intra-arterial injected contrast medium through animal experiments. One limitation of animal experiments is that hemodynamic condition of the experimental animal is not always kept constant. After contrast medium injection into the animal, recirculation of the contrast medium throughout the animal body may contaminate results of subsequent experiment batches.<sup>2)</sup> In addition, according to ethical considerations in an animal experiment, if an animal experiment can be substituted by another experiment which does not involve the use of animals, carrying out the latter has been recommended.<sup>3)</sup> From this viewpoint, a DSA phantom as an inanimate system that closely simulates the human cerebral vascular system can aid in the understanding of the bolus geometry of intra-arterial injected contrast agent. An inanimate phantom can always maintain and control external confounding factors such as a constant heart rate, body temperature, and blood pressure. Therefore, we considered conducting a cerebrovascular phantom experiment that could control various confounding factors.

The development of a 3D printer has allowed us to make human-like phantom models accurately with little effort. To the best of our knowledge, a cerebrovascular phantom flow system that mimics a cerebral capillary system in a contrast media experiment has not been reported yet. The cerebrovascular phantom flow system lacking a mimicking cerebral capillary system is the same as an arteriovenous shunt system that is directly connected to the artery and vein. In the absence of a mimicking capillary system, it is difficult to describe the actual cerebrovascular system. A new type of cerebral phantom flow system without shunt flow was needed to study contrast concentration change and cerebral circulation time.

We hypothesized that a well-mimicking artificial capillary bed can serve as optimal resistance for cerebrovascular phantom flow system and mimic the actual transit time in the arterial vasculature. Thus, we designed an in vitro intracranial arterial phantom flow system with a mimicking capillary system for studying changes in contrast medium concentration. To validate the cerebrovascular phantom model, we verified arterial contrast concentration of this model compared with that of a real patient's cerebral vasculature. This was validated using color-coded DSA. Syngo iFlow was used as the color-coding tool (Siemens, Erlangen, Germany) of 2D-DSA acquisitions. The color-flow image was related to the transit time.<sup>4)</sup> It can create a contrast concentration–time curve of a contrast medium bolus at a selected location on 2D-DSA images.

The objective of this study was to make an optimized cerebral DSA phantom to mimic the DSA image of actual neuro-angiography and demonstrate that the neuro-angiography vascular phantom flow system could simulate the contrast concentration–time curve pattern similar to that of a real human cerebral artery.

## **MATERIALS AND METHODS**

### **Selection of a patient model**

We selected a young patient who was diagnosed with a small middle cerebral artery (MCA) aneurysm to construct a cerebrovascular phantom model. Chronic headache led him to undergo magnetic resonance angiography. There was an incidental finding of MCA aneurysm. An intra-arterial catheter angiography was performed to accurately evaluate the aneurysm morphology. Exclusion criteria for creating a cerebrovascular phantom model were the presence of intracranial stenosis, arteriovenous fistula, and arteriovenous malformation. Our patient only experienced an aneurysm without other diseases.

An Artis zee biplane (Siemens, Erlangen, Germany) angiography suite was used for intra-arterial catheter angiography. We placed a 4F diagnostic angio-catheter (Jungsung Inc., Seoul, Korea) at the level of C3-C4 vertebral body for DSA imaging. We injected 8 mL of a contrast medium (Visipaque, iodine 270 mg/ml; GE healthcare, Chicago, Illinois) at 4 mL/s using a power injector (Medrad Mark V ProVis; Bayer, Leverkusen, Germany) for 2D angiography. For 3D angiography, we injected 15 mL of the contrast medium (270 mgI/mL) at 2.5 mL/s. This contrast injection protocol was equally applied to experiments in the cerebrovascular phantom flow system.

### **Image processing with iFlow**

Quantitative measurements of contrast concentration change can be made over time in the cerebral artery using image processing software (syngo iFlow; Siemens, Erlangen, Germany). According to the time to maximum point of contrast concentration, iFlow was used to make 2D color code DSA (Figure 1). A cerebral angiography was performed in iFlow mode. DSA images for iFlow were serially obtained at 7.5 frames/s over a period of 4 s, 4 frames/s for 6 s, and 2 frames/s. We avoided the location of vessel overlaps for measurement because it could

result in heterogenous attenuation instead of homogeneous attenuation. In addition, we focused on an intradural location. Consequently, change in contrast concentration in terminal internal carotid artery (ICA) on the frontal plane was measured to prevent measurements at sites overlapping with other vascular structures.

### **Construction of the cerebrovascular phantom model**

We obtained the patient's 3D angiography data and created an *in vitro* model of intracranial artery including the MCA aneurysm. After identifying the region of interest (ROI) to be modeled on 3D angiography images, the vessel was segmented by Hounsfield Units (HU) and 3D modeled using Mimics (Materialize, Leuven, Belgium), Meshmixer (Autodesk, San Rafael, United States), and Aview (Convergence Medicine, Asan Medical Center, Seoul, South Korea) software. Segmented vessel was converted to a stereolithography file format for 3D printing (Figure 2A).

The cerebrovascular phantom model resembling the intracranial artery of a real patient was constructed using a 3D printer (Zortrax M200, Zortrax S.A., Lubelska, Poland). The structure of the model was printed with Acrylonitrile Butadiene Styrene copolymer at a resolution of 90–390 microns. The surface of the output was finished with acetone. We used sandpaper and varnish solution to trim the 3D printed vascular model. The varnish solution filled irregular fine grooves of a vascular model surface. We immersed the vascular model in a container containing liquid silicon (Figure 2B). After the silicon solidified, the silicon was cut out to remove the vascular model. Finally, the hollow silicon mold was formed (Figures 2C, 2D). We injected molten wax into the silicon mold to obtain a vascular wax model. We then applied a thin layer of silicon to the wax model approximately five times. The silicon-coated wax model was placed in a rectangular silicon housing (Figure 2E). We punched holes in the silicon housing to connect it with the silicon-coated wax model. Transparent jelly-type silicon was then poured into the silicon housing to complete the hexahedron cerebrovascular phantom, after which the mold was placed in an oven to melt the wax. Finally, we obtained a

cerebrovascular phantom that was hollowed out in the shape of the patient's cerebral artery (Figure 3).



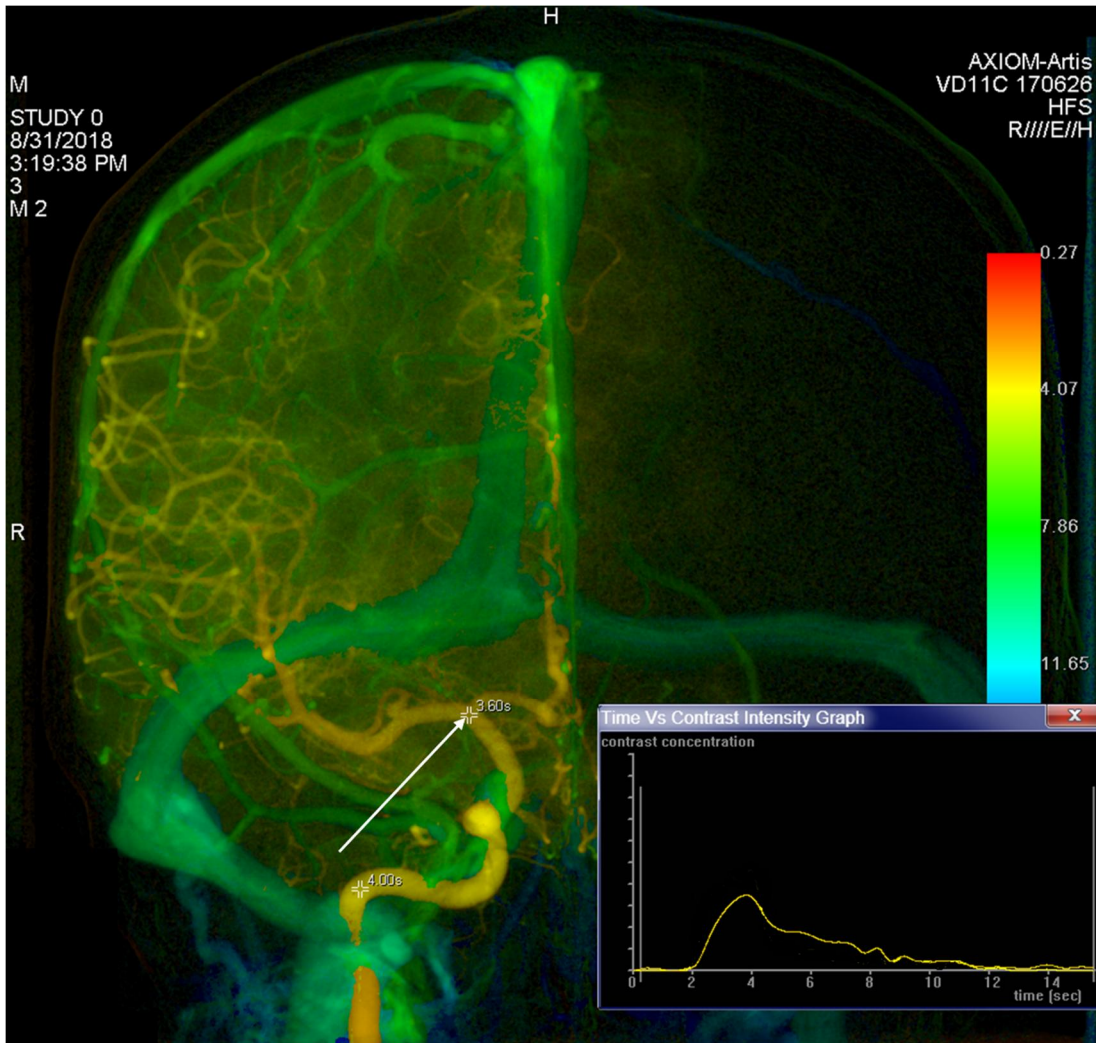


**Figure 1.** Region of interest at color coded digital subtraction angiography on AP view.

The contrast concentration was measured at terminal ICA (white arrow) on AP view.

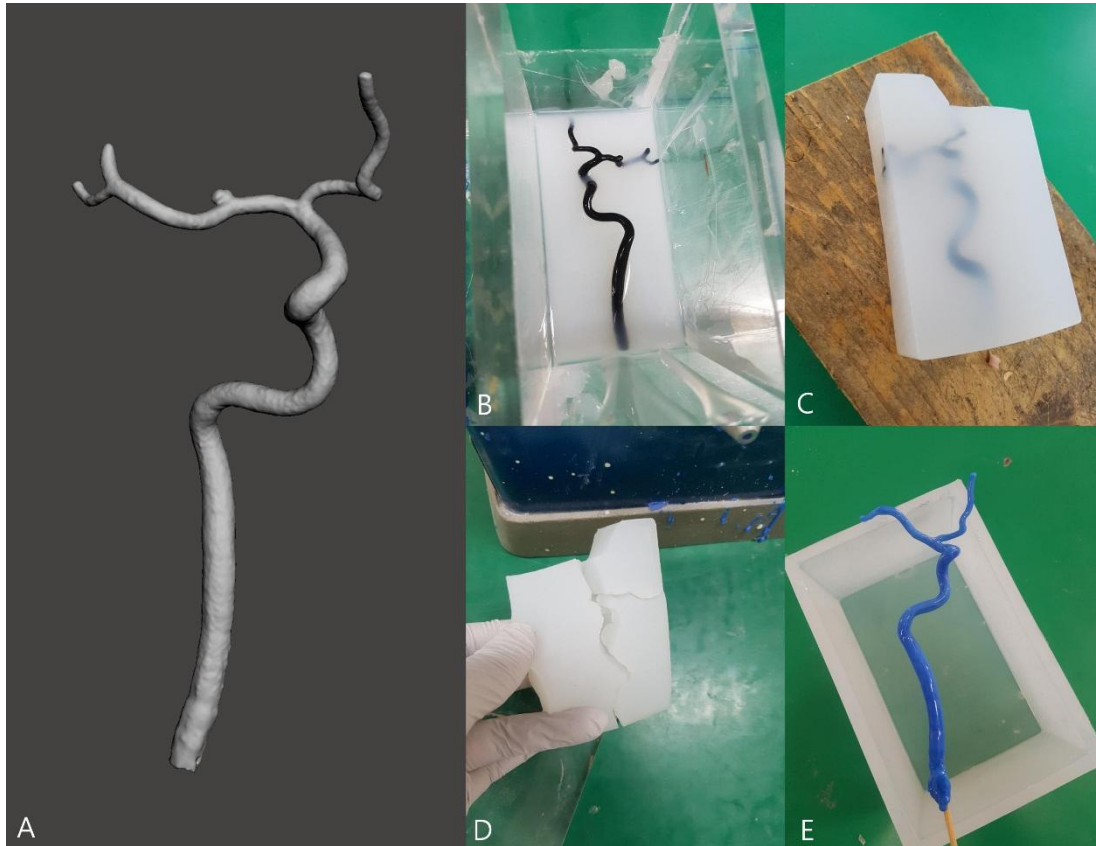


**Figure 2.** Construction of a cerebrovascular phantom.

A. A 3D vessel image in a stereolithography file format for 3D printing.

B. A 3D printed vascular acrylonitrile butadiene styrene copolymer model in a container containing liquid silicon

C, D. Cutting out the silicon to remove the 3D printing model

E. The silicon-coated wax model was placed in a rectangular silicon housing.

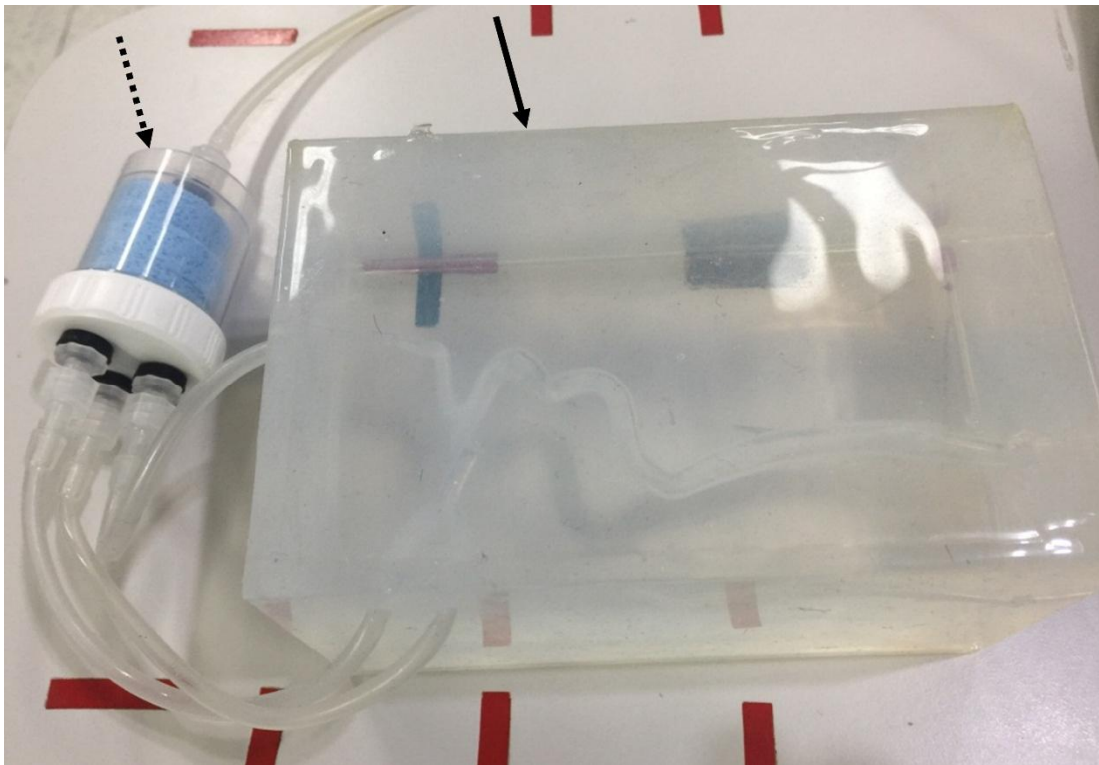


**Figure 3.** A cerebrovascular phantom model (black arrow) with an artificial brain capillary system.

The resistance module of cerebrovascular phantom flow system was composed of a plastic cistern filled with sponge (black dotted arrow).

### **Configuration of the cerebrovascular phantom flow system**

Our cerebrovascular phantom flow system consisted of a cerebrovascular phantom model, an acrylic hollow cistern filled with sponge, a pump, an injection system, a pressure-monitoring system, a constant temperature bath, and a venous drainage container. The entire cerebrovascular phantom system is shown in Figure 4. Water was transferred from a constant temperature bath (BW-05G; Lab Companion, Seoul, Korea) to the venous drainage container by a peristaltic pulsating flow pump (Ecoline VC-380; ISMATEC, Wertheim, Germany). We measured physiologic parameters (viscosity, blood pressure, pulse rate, body temperature) of the actual patient and used them as input data for the cerebrovascular phantom flow system. The peristaltic pump for pulsatile flow was controlled to show a pulse rate of 60 beats/min and a systolic pressure of 100 mmHg in the phantom flow system, similar to those of the patient. A 40:60 glycerol/water mixture for fluid viscosity of the phantom flow system was prepared by weight as working fluid.<sup>5)</sup> Dynamic viscosities of the actual patient's blood and working fluid of the phantom flow system were  $3.00 \times 10^{-3}$  kg/m·s and  $3.22 \times 10^{-3}$  kg/m·s, respectively. We implemented venous sinus pressure of approximately 10 cm H<sub>2</sub>O by elevating the venous drainage container at 10 cm above the overall system height. Contrast material was injected via a 4F catheter with a power injector (Medrad Mark V ProVis; Bayer, Leverkusen, Germany), similar to the contrast injection protocol used for the patient.

We used a plastic cistern filled with sponge to represent the mimicking capillary system. The density of the sponge was  $1.76 \mu\text{g}/\text{mm}^3$ . The mimicking capillary system was designed to control the resistance of the phantom flow system. We defined the system types as follows: Type A, the mimicking capillary system was not incorporated into the phantom flow system; Type B, with incorporation of plastic cistern only; and Type C, with incorporation of a plastic cistern filled with sponge. Subsequently, we compared iFlow measurements among these three groups.

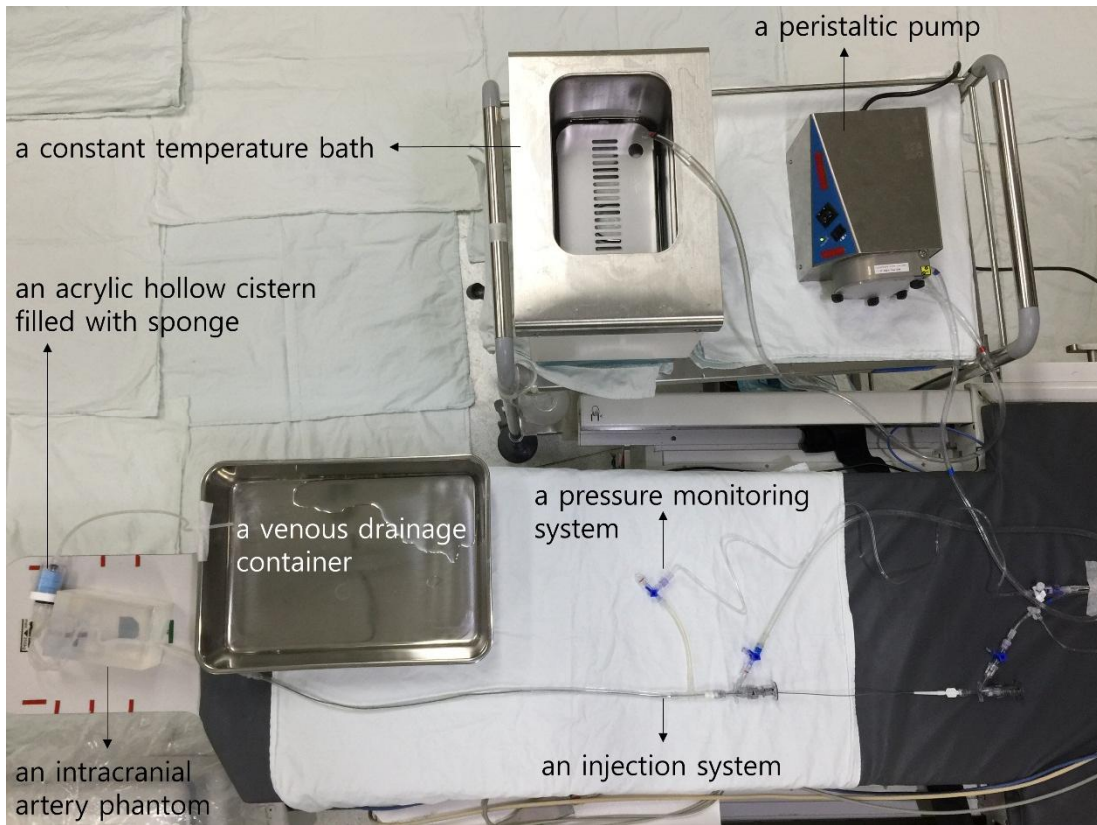


Figure 4. The entire cerebrovascular phantom flow system.

## **Validation of cerebrovascular phantom flow system**

To validate the cerebrovascular phantom flow system, we compared iFlow contrast concentration–time curve pattern of the real patient with that of the cerebrovascular phantom flow system. The real patient’s angiography iFlow data were used as reference for phantom experiments. The arterial vasculature of the patient and that of a phantom model had similar X-ray projection angle and catheter position in intra-arterial catheter-based angiogram. Hence, iFlow images could be obtained at the same frame rate and projection angle.

The contrast concentration–time curve obtained from iFlow data is a non-linear curve because the flow in arterial vessels is both temporally and spatially inhomogeneous.<sup>6)</sup> Therefore, it is difficult to quantitatively analyze similarity between contrast concentration–time curves. Thus, four parameters were adopted for analysis of iFlow images: 1) maximum contrast concentration, 2) time to peak (TTP), 3) full width at half maximum, and 4) area under curve (AUC) (Figure 5). First, we compared maximum contrast concentration values of the contrast concentration–time curves for quantitative analysis. The concept of “time to peak (TTP)” contrast concentration at the selected “region of interest (ROI)” was considered to illustrate contrast concentration temporal change in arterial vasculature. TTP parameter was used for time analysis.<sup>4)</sup> TTP was defined as the time when maximum X-ray attenuation owing to contrast was attained along angiographic series. The reference time,  $t = 0$ , was defined as the time of mask appearing. We took the first frame before contrast at the start of the viewing window. The last frame of the run was the end of the viewing window. We then considered the TTP that showed the time when the maximum value appeared in the time axis. We measured the full-half width and AUC to compare the wideness of the curve. The full width at half maximum was the time period when the contrast concentration reached half of the maximum value.

We repeated the experiment 10 times in the same ROI (terminal ICA on the frontal plane) of A, B, and C types to obtain median values for the four parameters of the patient’s contrast concentration–time curve. Subsequently, we compared these four parameters with those of phantom circuits with/without an artificial capillary system.

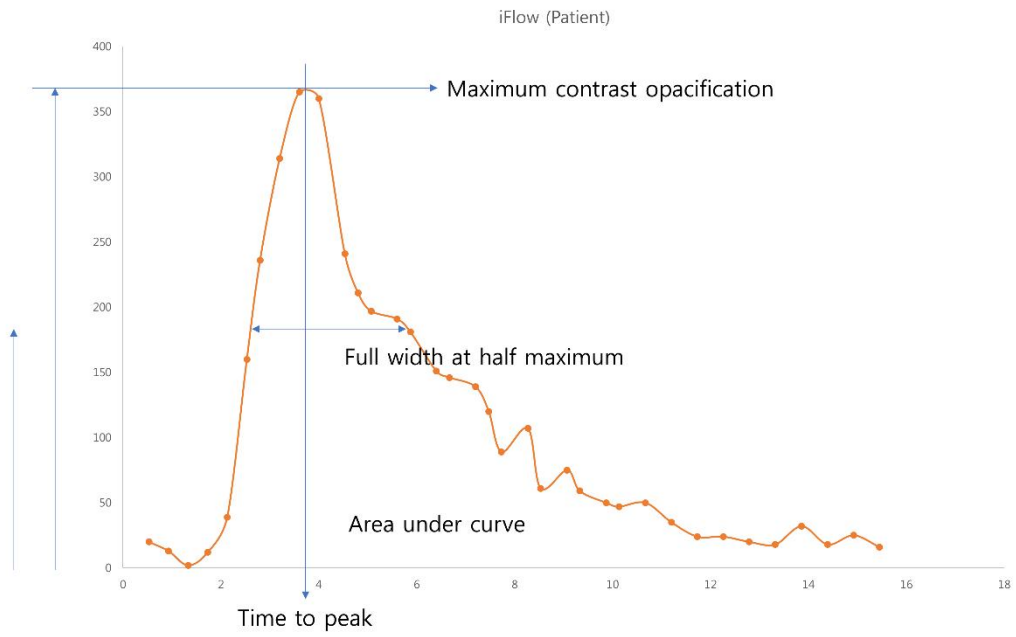


Figure 5. Four parameters (maximum contrast concentration, time to peak, full width at half maximum, and area under curve) were adopted for analyzing iFlow images.

### **Statistical analysis**

All statistical analyses were performed using Wilcoxon signed-rank test. Wilcoxon rank sum test was used to examine difference in each parameter between phantom models with/without an artificial capillary system. All statistical analyses were performed using IBM SPSS statistics software (IBM, Armonk, NY, USA).



## RESULTS

All four parameters for the assessment of change in contrast concentration showed a serial increase in values for Type A, Type B, and Type C (Table 1). We compared differences in each parameter value among the three groups.

For maximum contrast concentration (Figure 6a), median values for Type A, Type B, and Type C were 271.5, 364.5, and 390.0, respectively. The iFlow measurement of the patient showed the closest match with that of Type B ( $p$ -value = 0.168 in comparison with patient values). For TTP (Figure 6b), the median value was 3.54 s for Type A, 3.74 s for Type B, and 3.94 s for Type C. The patient score was 3.60 s, which was the most similar to the Type A score ( $p$ -value < 0.001 in comparison with patient value). For full width at half maximum (Figure 6c), the median value was 1.71 s for Type A, 1.87 s for Type B, and 2.34 s for Type C. The patient score was 3.22 s, which was the most similar to Type C score ( $p$ -value < 0.001 in comparison with patient value). In the case of AUC (Figure 6d), the median value was 657.23 for Type A, 993.58 for Type B, and 1572.83 for Type C. The patient score was 1519.55, which was the most similar to the Type C score ( $p$ -value < 0.001 in comparison with patient values).

Figure 7 shows contrast concentration–time curves for median values of contrast concentration measurements obtained from iFlow data for each group. They were compared with measurements of the contrast concentration–time curve plotted for the actual patient. We found that these contrast concentration–time curves became broader and the maximum values of curves increased when a mimicking capillary system was applied.

Table 1. The four parameters for contrast opacity temporal change in types A, B, and C.

	Patient	Type A <sup>†</sup> (n = 10)	<i>p-value</i> *	Type B <sup>‡</sup> (n = 10)	<i>p-value</i> *	Type C <sup>§</sup> (n = 10)	<i>p-value</i> *
Maximum contrast concentration							
Median (IQR)	365.00	271.50 (257.00 - 276.00)	<0.001	364.50 (351.00 - 377.00)	0.168	390.00 (383.00 - 411.00)	<0.001
(Min – Max)		(241.00 - 298.00)		(339.00 - 385.00)		(300.00 - 431.00)	
Time to peak							
Median (IQR)	3.60	3.54 (3.47 - 3.60)	<0.001	3.74 (3.60 - 3.87)	<0.001	3.94 (3.73 - 4.27)	<0.001
(Min – Max)		(3.33 - 3.73)		(3.47 - 4.00)		(3.73 - 4.27)	
Full width at half maximum							
Median (IQR)	3.22	1.71 (1.68 - 1.72)	<0.001	1.87 (1.77 - 1.96)	<0.001	2.34 (2.12 - 2.42)	<0.001
(Min – Max)		(1.61 - 1.82)		(1.70 - 2.10)		(1.98 - 4.15)	
Area under curve							
Median (IQR)	1519.55	657.23 (631.84 - 720.94)	<0.001	993.58 (909.79 - 1062.31)	<0.001	1572.83 (1492.73 - 1860.27)	<0.001
(Min – Max)		(592.36 - 752.22)		(809.90 - 1189.80)		(1313.38 - 1974.29)	

\* *p-value* in comparison with patient values according to Wilcoxon signed-rank test

<sup>†</sup> Type A did not incorporate the mimicking capillary system into the phantom flow system

<sup>‡</sup> Type B involved the incorporation of plastic cistern only

<sup>§</sup> Type C involved the incorporation of a plastic cistern filled with sponge

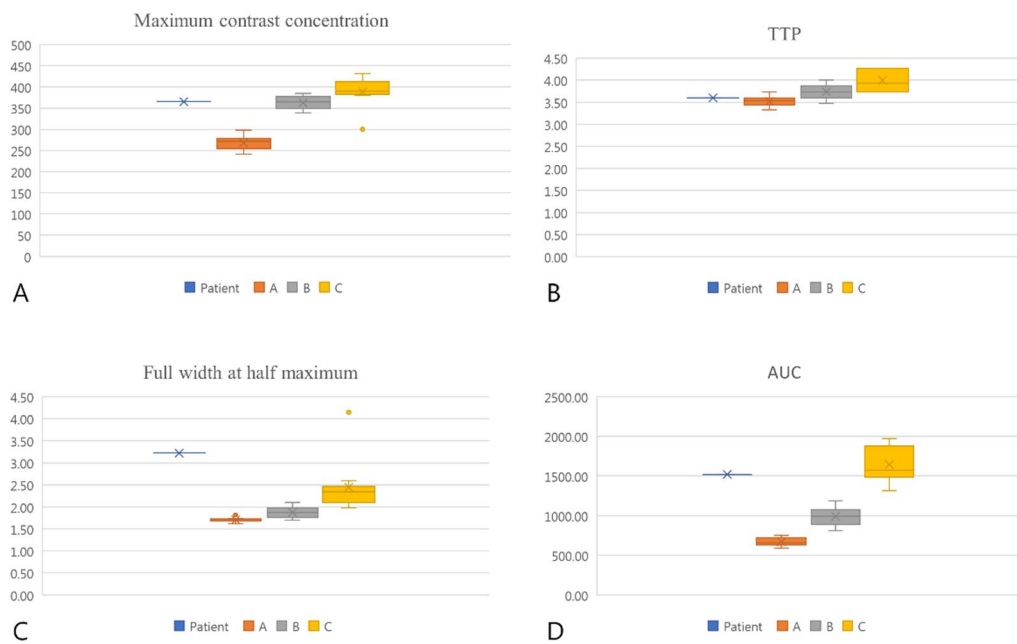


Figure 6. Comparisons among the four parameters for Types A, B, and C.

A. The maximum contrast concentration

B. Time to peak

C. Full width at half maximum

D. Area under curve

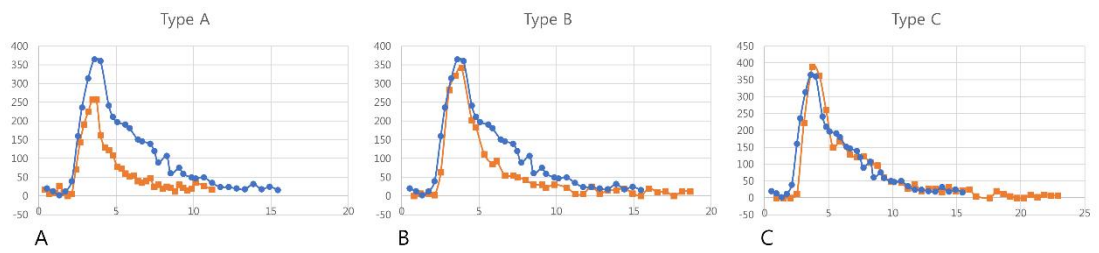


Figure 7. Comparisons between iFlow contrast concentration–time curves of the original person (blue line) and cerebrovascular phantoms (red line).

A. Comparison of the iFlow contrast concentration–time curve for Type A.

B. Comparison of the iFlow contrast concentration–time curve for Type B

C. Comparison of the iFlow contrast concentration–time curve for Type C.

## DISCUSSION

To the best of our knowledge, most cerebrovascular phantoms have not been able to simulate the cerebral capillary system of the brain parenchyma. We hypothesized that the cerebral capillary system would be a capacitor like spongy body that could receive blood from the arterial system. Thus, an acrylic hollow cistern filled with sponge was introduced to simulate the cerebral capillary system.

The iFlow application provided by Siemens angiosuite demonstrated time-dependent changes in contrast remaining in the large cerebral artery.<sup>6-8)</sup> These changes in contrast concentration occurred when the contrast agent in the large cerebral vessel lumen entered the capillary system of the brain. In this study, we tested the ability of a sponge-containing plastic cistern to actually simulate the capillary system of the brain in a cerebrovascular phantom flow system using iFlow application. We designed four parameters to quantitatively validate the phantom system. These parameters could be used for studying time-related change in contrast concentration in the cerebral artery. They were useful tools to quantitatively compare the similarity of the contrast concentration–time curve graph pattern. Among these four parameters, two parameters, namely full width at half maximum and AUC, in Type C showed maximum similarity with those of the patient’s contrast concentration–time curve (*p-value* < 0.001 in comparison with patient values). Moreover, to compare the overall graph pattern, we reconstructed contrast concentration–time curves as the median of measurement values extracted from contrast concentration–time curves of Type A, Type B and Type C. When comparing these curves with the actual patient's contrast concentration–time curves, we could see that Type C curve was more similar to the patient's curve. Hence, we decided to use the Type C model for studying changes in contrast concentration associated with catheter-based angiography in the future. We expected to use our cerebrovascular phantom flow system for analyzing factors affecting the contrast media concentration of the cerebral artery in future studies.

Each cerebral disease has various patterns of angiographic cerebral circulation time. Through extensive investigations of cerebral arteriography for diseases such as atherosclerosis and thrombotic cerebral vascular disease, we have observed a considerable delay in contrast opacification of small cerebral arteries.<sup>9)</sup> A study on an occlusive internal carotid artery lesion has suggested that angiographic cerebral circulation time and cerebral vasoreactivity are well correlated.<sup>10)</sup> A recent study on multiple sclerosis has demonstrated that there is a significant difference in cerebral circulation time between multiple sclerosis patients (mean = 4.9 s; sd = 1.27 s) and normal control subjects (mean = 2.8 s; sd = 0.51 s), This suggests that an increased cerebral circulation time in multiple sclerosis patients means microvascular dysfunctions.<sup>11)</sup> Another study has shown that there are differences in cerebral circulation time between hemorrhagic and non-hemorrhagic Moyamoya disease patients.<sup>12)</sup> The cerebral circulation time of the contrast may vary depending on the degree of cerebral perfusion in the brain parenchyma. Recent studies on dementia have investigated cerebral perfusion in the brain parenchyma.<sup>13-15)</sup> The cerebral circulation time can be obtained by measuring the contrast concentration in cerebral angiography. It is thought to be closely related to the contrast concentration–time curve. By adjusting the transition time of the phantom flow system to reproduce the characteristic cerebral circulation time of each disease group, we can create a phantom flow system that can aid in the study of each disease. The *in vitro* phantom model constructed in this study might help us understand the physiologic phenomenon of brain perfusion.

We demonstrated that the iFlow pattern of the phantom could be adjusted to be similar to that of the patient by adding a sponge to the plastic cistern. When creating an *in vitro* cerebrovascular phantom flow system, the key point is how much resistance should be given to the circuit. The cerebrovascular phantom flow system attached to an artificial capillary device could be expected to simulate the brain perfusion pattern because the transit time of the intra-arterial vasculature can be controlled by adjusting the resistance of the phantom circuit. It would be a future task to quantitatively express and control resistance in the phantom flow circuit.

Although studies on computational fluid dynamics (CFD) associated with cerebral blood vessels have been actively conducted so far, validating results with those of real human being has been challenging.<sup>16-18)</sup> It is impossible to obtain repetitive measurements of hemodynamic parameters through *in vivo* tests because of human ethical considerations. In this regard, validation using a cerebrovascular phantom flow system that simulates a real cerebrovascular system can be another solution. The phantom flow system used in this study is an updated system mimicking the capillary system of a real person. It is necessary to test whether the hemodynamics in an arterial system can be similarly implemented in a real human being when contrast concentration–time curves of a phantom model and a real person are similar. Cerebral circulation time and cerebral blood flow are known to show significant correlation.<sup>19)</sup> This, if measurements of hemodynamic parameters in an actual vascular system are consistent with measurements obtained from the phantom, this updated cerebrovascular phantom flow system could be helpful in CFD validation. Additionally, future research on the correlation between contrast concentration time curves and hemodynamic parameters such as flow rate and pressure might allow iFlow to be used as a good tool for CFD validation.

### **Limitations**

First, iFlow data during only one DSA run was considered acceptable for the evaluation of the patient's aneurysm. This meant that the real patient's iFlow data was obtained only once in order to avoid causing any disturbance of experimental ethics. In other words, the iFlow reference data of the person to be compared with the iFlow value obtained from the phantom experiment was the value obtained from only one DSA run. However, this situation was inevitable considering the ethics of human experimentation which in turn reflects the importance of the phantom experiment in this study.

Second, to analyze iFlow data in detail, the number of frames per second should be high. However, keeping human ethical considerations in mind, it was necessary to use a small number of frames in order to prevent the patient from receiving an increased radiation dose

during DSA. We believed that we had enough frames to analyze the iFlow data for our contrast study.

Third, we did not use a cylinder type pump in the phantom flow system. The peristaltic pump can produce pulse pressure. However, it does not show similar hemodynamic curve from the arterial pressure monitoring that can be obtained in the human body.



## **CONCLUSION**

Our neuro-angiography vascular phantom flow system was designed to study changes in the contrast medium concentration in catheter-based cerebral arteriogram. We believe that the study of cerebrovascular phantom flow system can be preferred over other study modalities considering the limitation of animal models and the unethical nature of human experiments. We demonstrated that the contrast concentration–time curve of a real patient could be simulated in the phantom model by adjusting resistance of the phantom flow system through an acrylic hollow cistern filled with sponge. In this study, we developed a methodology to compare similarities of various contrast concentration–time curves characterized by iFlow application. Our study on cerebrovascular phantom flow system also provided a methodological foundation for contrast study in catheter-based cerebral arteriogram.

## REFERENCES

1. Ahmed AS, Deuerling-Zheng Y, Strother CM, et al. Impact of intra-arterial injection parameters on arterial, capillary, and venous time-concentration curves in a canine model. *AJNR Am J Neuroradiol.* 2009;30(7):1337-41.
2. Burbank FH, Brody WR, Bradley BR. Effect of volume and rate of contrast medium injection on intravenous digital subtraction angiographic contrast medium curves. *J Am Coll Cardiol.* 1984;4(2):308-15.
3. Ghasemi M, Dehpour AR. Ethical considerations in animal studies. *J Med Ethics Hist Med.* 2009;2:12.
4. Strother CM, Bender F, Deuerling-Zheng Y, et al. Parametric color coding of digital subtraction angiography. *AJNR Am J Neuroradiol.* 2010;31(5):919-24.
5. Ha H, Hwang D, Kim GB, et al. Estimation of turbulent kinetic energy using 4D phase-contrast MRI: Effect of scan parameters and target vessel size. *Magn Reson Imaging.* 2016;34(6):715-23.
6. Lin CJ, Hung SC, Guo WY, et al. Monitoring peri-therapeutic cerebral circulation time: a feasibility study using color-coded quantitative DSA in patients with steno-occlusive arterial disease. *AJNR Am J Neuroradiol.* 2012;33(9):1685-90.
7. Cover KS, Lagerwaard FJ, van den Berg R, et al. Color intensity projection of digitally subtracted angiography for the visualization of brain arteriovenous malformations. *Neurosurgery.* 2007;60(3):511-4; discussion 4-5.
8. Lin CJ, Luo CB, Hung SC, et al. Application of color-coded digital subtraction angiography in treatment of indirect carotid-cavernous fistulas: initial experience. *J Chin Med Assoc.* 2013;76(4):218-24.
9. Gotham JE, Gilroy J, Meyer JS. Studies of cerebral circulation time in man. 1. Normal values and alterations with cerebral vascular disease and tumour in arm-to-retina circulation times. *J Neurol Neurosurg Psychiatry.* 1962;25:292-302.
10. Yamamoto S, Watanabe M, Uematsu T, et al. Correlation of angiographic circulation

- time and cerebrovascular reserve by acetazolamide-challenged single photon emission CT. *AJNR Am J Neuroradiol.* 2004;25(2):242-7.
11. Monti L, Donati D, Menci E, et al. Cerebral circulation time is prolonged and not correlated with EDSS in multiple sclerosis patients: a study using digital subtracted angiography. *PLoS One.* 2015;10(2):e0116681.
  12. Kang K, Lu J, Zhang D, et al. Difference in cerebral circulation time between subtypes of Moyamoya disease and Moyamoya syndrome. *Sci Rep.* 2017;7(1):2587.
  13. Fallmar D, Lilja J, Velickaite V, et al. Visual assessment of brain perfusion MRI scans in dementia: a pilot study. *J Neuroimaging.* 2016;26(3):324-30.
  14. de Roos A, van der Grond J, Mitchell G, Westenberg J. Magnetic resonance imaging of cardiovascular function and the brain: is dementia a cardiovascular-driven disease? *Circulation.* 2017;135(22):2178-95.
  15. Wolters FJ, Zonneveld HI, Hofman A, et al. Cerebral perfusion and the risk of dementia: a population-based study. *Circulation.* 2017;136(8):719-28.
  16. Hariharan P, D'Souza GA, Horner M, et al. Use of the FDA nozzle model to illustrate validation techniques in computational fluid dynamics (CFD) simulations. *PLoS One.* 2017;12(6):e0178749.
  17. Paliwal N, Damiano RJ, Varble NA, et al. Methodology for computational fluid dynamic validation for medical use: application to intracranial aneurysm. *J Biomech Eng.* 2017;139(12).
  18. Bouillot P, Brina O, Ouared R, et al. Computational fluid dynamics with stents: quantitative comparison with particle image velocimetry for three commercial off the shelf intracranial stents. *J Neurointerv Surg.* 2016;8(3):309-15.
  19. Aikawa H, Kazekawa K, Tsutsumi M, et al. Intraprocedural changes in angiographic cerebral circulation time predict cerebral blood flow after carotid artery stenting. *Neurol Med Chir (Tokyo).* 2010;50(4):269-74.

## 국문요약

**배경 및 목적:** Cerebrovascular flow, pressure 등을 측정하여 shear stress 등의 hemodynamic flow를 묘사하는 연구는 많으나 Cerebral circulation과 연관된 contrast media에 관한 연구는 그리 많지 않았다. 특히 contrast의 변화를 연구한 이전의 실험 들에서 모세혈관계를 묘사한 system은 없었다. 모세혈관계가 없는 phantom flow system은 동맥과 정맥이 바로 연결되어 있는 arteriovenous shunt system이기에 실제 뇌혈관계를 묘사하였다 보기 힘들고 실제 조영제의 변화 양상을 묘사하기 힘들다. 따라서 본 연구에서는 뇌혈관 조영술 시 뇌동맥에서의 시간당 contrast 농도 변화에 영향을 미치는 모세혈관계의 역할을 위한 인공 장치를 고안 후 이를 평가하였다.

**연구 방법:** Vascular phantom은 Siemens angiosuite에서 얻은 Digital Subtraction Angiography 3D data를 통해 3D printer로 출력된 입체물을 기반으로 실리콘을 재료로 하여 제작되었다. 모세혈관계는 해면체와 같이 혈액을 머금고 있는 상태에서 동맥계로부터 혈액을 받아들인다 가정하였고 이를 가장 잘 묘사할 수 있는 재료로 해면 스펀지와 같은 인공 스펀지를 선정하였다. 이를 이용해 인공 모세혈관 module을 만들어 이를 phantom과 연결하여 flow system을 구성하였다. 그리고 이 flow system이 모세혈관계를 실제로 묘사할 수 있는지 Siemens angiosuite의 iFlow를 통해 검증을 하였다.

**연구 결과:** Siemens iFlow는 지정된 지점의 시간에 따른 contrast의 양의 변화를 보여주기에 phantom model에서 모세혈관계에 흡수되기 전 뇌동맥계에 잔류되는 contrast의 시간 당 변화를 보여줄 수 있었다. 또한 이를 이용해 스펀지를 이용한 인공 모세혈관계를 장착한 phantom flow system이 실제 환자의 iFlow pattern과 유사한 pattern을 보여줌을 실증하였다.

**연구 결론:** 인공 스펀지를 이용해 만든 인공 뇌모세혈관계를 통해 실제 인체의 cerebral circulation time을 모사하는 phantom flow system을 만들 수 있었다.

(중심단어: 뇌혈관조영술, 모세혈관계, 조영제, 팬텀)